NANO LETTERS

Letter

pubs.acs.org/NanoLett

Intrinsic Bauschinger Effect and Recoverable Plasticity in Pentatwinned Silver Nanowires Tested in Tension

Rodrigo A. Bernal,[†] Amin Aghaei,[‡] Sangjun Lee,[§] Seunghwa Ryu,[∥] Kwonnam Sohn,[⊥] Jiaxing Huang,[⊥] Wei Cai,*[,‡] and Horacio Espinosa*[,†]

[†]Department of Mechanical Engineering, Northwestern University, Evanston, Illinois 60208, United States

[‡]Department of Mechanical Engineering, Stanford University, Stanford, California 94305-4040, United States

[§]Department of Physics and [∥]Department of Mechanical Engineering, Korea Advanced Institute of Science and Technology (KAIST), Daejeon 305-701, South Korea

[⊥]Department of Materials Science and Engineering, Northwestern University, Evanston, Illinois 60208, United States

S *Supporting Information*

ABSTRACT: Silver nanowires are promising components of flexible electronics such as interconnects and touch displays. Despite the expected cyclic loading in these applications, characterization of the cyclic mechanical behavior of chemically synthesized high-quality nanowires has not been reported. Here, we combine in situ TEM tensile tests and atomistic simulations to characterize the cyclic stress−strain behavior and plasticity mechanisms of pentatwinned silver nanowires with diameters thinner than 120 nm. The experimental measurements were enabled by a novel system allowing displacement-controlled tensile testing of nanowires, which also affords higher resolution for capturing stress−strain curves. We observe the Bauschinger effect, that is, asymmetric plastic flow, and partial recovery of the plastic deformation upon unloading. TEM observations and atomistic simulations reveal that these processes occur due to the pentatwinned structure and emerge from reversible dislocation activity. While the incipient plastic mechanism through the nucleation of stacking fault decahedrons (SFDs) is fully reversible, plasticity becomes only partially reversible as intersecting SFDs lead to dislocation reactions and entanglements. The observed plastic recovery is expected to have implications to the fatigue life and the application of silver nanowires to flexible electronics.

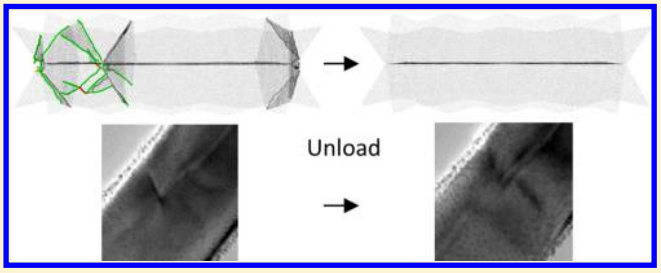

KEYWORDS: *Flexible electronics, displacement control, fatigue, nanoscale plasticity, cyclic straining*

Silver nanowires are being investigated as the conductive elements in flexible electronic systems. Because of their high conductivity and ease of synthesis, they have been employed in diverse applications such as high-conductivity flexible interconnects,[1] mechanically tunable antennas,[2] and strain sensors.[3] Furthermore, transparent conductive films employing silver nanowires, either embedded in transparent polymers or mixed with graphene to improve film conductivity,[4] have been deemed an important alternative to indium−tin oxide (ITO) in touch displays.[5] This technology has the potential to dramatically reduce costs in display technologies by replacing ITO, whose cost has increased due to scarce indium supply.[6] This potential is demonstrated by recent industrial interest in silver-nanowire-based conductive films.[7]

In all these flexible electronics applications, a random network of silver nanowires provides a conductive path for electrical signals. A reliable conductivity is dependent on the integrity of such network, which in turn is directly related to the mechanical integrity of the nanowires. As such, understanding the mechanical properties of silver nanowires is critical to predict failure modes of flexible electronic devices. In particular, due to continuous flexing of the electronic device and the random characteristic of the embedded nanowire network, it is reasonable to assume that silver nanowires may become stretched beyond the plastic limit and undergo several loading modes on repeated occasions, such as tension, compression, bending and buckling.

However, characterization of the mechanical properties of nanowires has mainly been reported in monotonic loading. Some examples of cyclic loading have been reported for microscale specimens, for example,[8−10] and only very recently for nanowires of sub-100 nm diameter in compression.[11,12] In fact, cyclic-straining experiments on sub-100 nm nanowires in tension have not been reported. As a result, little information is available on the deformation mechanisms that may emerge on nanosized metals from nonmonotonic loading beyond the plastic limit.

Received: August 22, 2014
Revised: October 1, 2014
Published: October 3, 2014

Beyond this application-driven need for mechanical characterization, there is a fundamental interest in the understanding of plastic deformation mechanisms present in sub-100 nm metal structures. This interest arises due to the observation of increasing yield-strength with decreasing sample size, attributed to the transition from a regime controlled by dislocation motion to one controlled by dislocation nucleation.[13−15] Similarly, the mechanisms of cyclic plastic deformation and dislocation accumulation, which presumably control the fatigue behavior of these specimens, have not been explored yet.

In this work, we carry out a combined experimental−computational approach to study the behavior of silver nanowires past the plastic limit on repeated loading−unloading tensile cycles. We demonstrate that the nanowires recover a fraction of the plastic deformation upon unloading. The fraction of plastic recovery increases with increasing strain, and also increases slightly with decreasing nanowire diameter. These observations can be explained by reversible dislocation mechanisms identified through atomistic simulations.

Combined Experimental-Computational Approach. Silver nanowires with a pentatwinned structure were chemically synthesized and characterized extensively by HRTEM as reported elsewhere.[14] Nanowire diameter ranges approximately from 30 to 120 nm with lengths of several microns. The nanowires consist of five single crystal domains, all aligned in the ⟨110⟩ directions and intersecting at {111} twin boundaries. Recent reports have established that these nanowires display increasing tensile strength with decreasing diameter[14,16] and distributed plastic deformation that delays localization.[14] Plasticity is initiated by the nucleation of Shockley partial dislocations from the nanowire surface, which lead to the formation of 5-fold stacking fault decahedrons (SFD), as predicted by molecular dynamics (MD) simulations. The signature of multiple SFD chains was also observed by in situ TEM experiments.[14] The first SFD catalyzes the formation of a chain of SFDs along the nanowire until the process stops due to diameter variations, and plasticity can be reinitiated by forming another chain of SFDs at a different location on the nanowire.

The loading conditions in previous tensile tests of nanowires,[17−21] including ours,[22] can be described as in-between force-controlled and displacement-controlled. As a result, the coupling between the loading mechanism and the deformation processes in the sample makes the analysis difficult. On the other hand, strict displacement control matches closely the loading condition of atomistic simulations and allows detection of individual yield events.[23] In this work, we utilize a recently developed testing system based on microelectromechanical system (MEMS) technology (Figure 1a), which permits fully instrumented uniaxial tensile testing of nanowires in displacement control with high signal-to-noise ratio.[24] In the testing microsystem, the flexible element used to measure load is kept stationary by means of closed-loop feedback control (hardware-based) and electrostatic actuation. This feedback control prevents accumulation of elastic energy in the testing microsystem.

The operation of the tensile testing device can be understood as follows.[24] As voltage is applied to the thermal actuator with chevron beams,[25] Joule heating causes deformation of the beams, moving a shuttle where one end of the specimen is positioned (Figure 1b). This actuator therefore controls the strain applied to the specimen. The sample is attached on the other end to a load sensor, where a capacitance change proportional to the sensor displacement is generated and

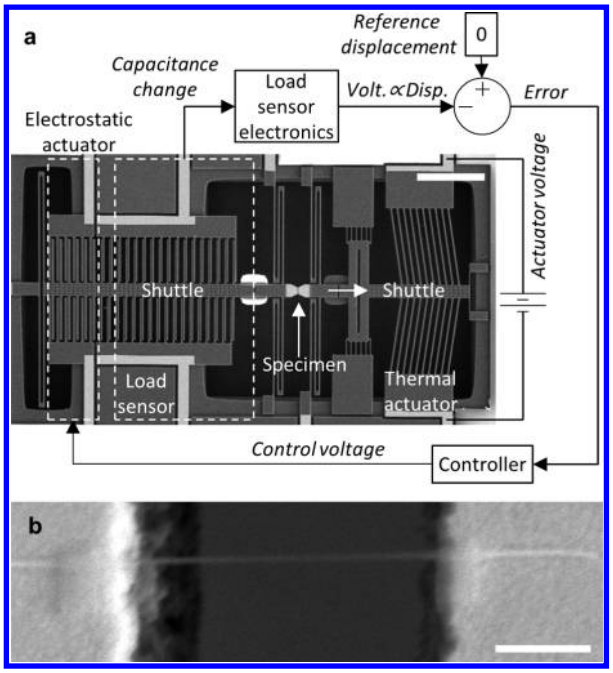

Figure 1. Experimental tensile testing of nanowires. (a) SEM micrograph and electronic schematic of the MEMS for displacement-controlled testing of nanowires. Scale bar: 300 μm. (b) SEM micrograph of one of the nanowires tested (diameter: 38 nm). Scale bar: 1 μm.

converted to a voltage. This voltage is compared to a reference corresponding to the displacement-control condition (i.e., zero voltage), and the difference (error) is fed to a controller, which computes a control voltage applied to the electrostatic actuator, in order to keep the load sensor stationary. The electrostatic force is equal to the force in the specimen, which can then be computed from the applied voltage and the actuator geometry. The implementation of closed-loop feedback control, plus the fabrication of the device by silicon-on-insulator (SOI) technology with a device layer 25 μm thick, leads to a high resolution on the stress−strain curves capable of capturing sudden unloading events associated with the nucleation of dislocations from the surface of the nanowires. This is exemplified on the stress−strain curve plotted in Figure 2a and stress−strain curves presented in the Supporting Information for wire diameters in the range of 38−118 nm. This device therefore allows unprecedented resolution in mechanical testing of sub-100 nm nanowires, combined with tensile loading, which is preferred over compression due to potential in-homogeneities on compressive loading near the indenter punch.[13]

Tensile testing of silver nanowires was carried out under in situ scanning electron microscopy (SEM). Cyclic straining was achieved by performing several loading unload−reload cycles with increasing unloading strain, up to fracture. Six nanowires were experimentally tested, ranging from 38 to 118 nm in diameter. The strain rate throughout the tests was kept constant at approximately 1.5×10^{-3}/s. For details on data reduction and electronics, please see Methods section. A separate experiment in situ transmission electron microscopy (TEM) was used to elucidate atomistic mechanisms.

To compare with experiments and gain atomistic insights we performed loading−unloading molecular dynamics simulations using the MD++[26] and LAMMPS[27] codes on nanowires with

dx.doi.org/10.1021/nl503237t | Nano Lett. 2015, 15, 139−146

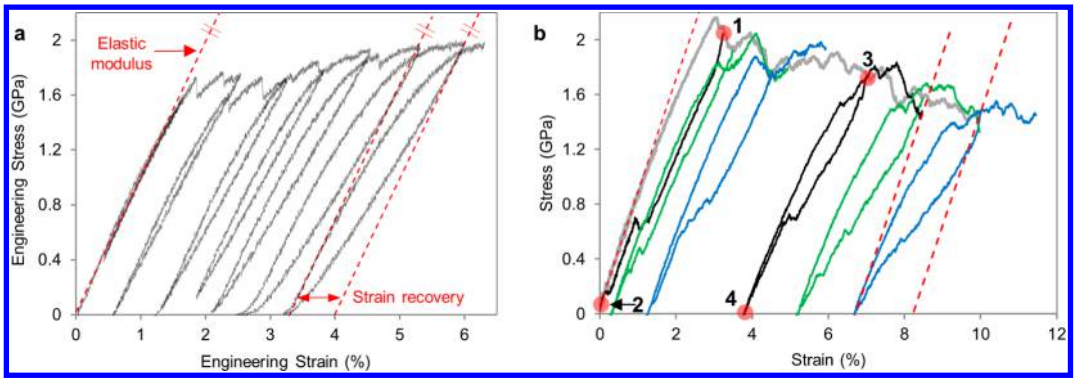

Figure 2. Representative stress–strain curves under repeated unload–reload cycles. The strain recovery is defined as the difference between the strain at zero stress if ideal elastic unloading happens (dashed lines) and the actual strain at zero stress. (a) Experimental curve for a 85 nm nanowire (b) MD simulation of an undulated 22 nm nanowire. Gray line corresponds to the first loading starting from the relaxed configuration until the strain reaches ~10%. Color lines correspond to unloadings and subsequent reloadings. Points 1–4 indicate points in the curve further analyzed in Figure 5.

diameters ranging from 6 to 22 nm and length to diameter ratio of about 2.5. We employ the embedded atom method (EAM) potential developed by Williams, Mishin, and Hamilton for silver.[28] The largest nanowire modeled consists of ~1 200 000 atoms. To mimic the diameter variation and surface roughness in the experimentally tested nanowires[14] the size of the pentagon-shaped cross section has a sinusoidal variation along the nanowire (see Figure 5).[29] The nanowires are then relaxed under the NPT ensemble at 300 K and zero axial stress for 100 ps. The nanowires are then loaded or unloaded along the long axis, both at a constant strain rate of 5×10^7/s. The temperature is kept at 300 K by the Nosé–Hoover thermostat during the whole loading–unloading process.

Cyclic Stress–Strain behavior: Strong Intrinsic Bauschinger Effect. Figure 2 shows representative stress–strain curves of the cyclic behavior of the nanowires for (a) experiments and (b) MD simulations (for more experimental stress–strain curves see Supporting Information). Both experimental and computational curves show hysteresis upon unloading and subsequent reloading, and the hysteresis increases as the unloading strain is increased. The hysteresis appears because the unloading portion of the curves differs significantly from the ideal elastic unloading (dashed lines), indicating that plastic flow occurs during unloading. It is encouraging to note that the atomistic simulations predict hysteresis-loop sizes that are similar to those observed experimentally. The softening behavior observed in MD simulations may be caused by the very high strain rate and limited size of the simulations, as hypothesized before.[14] However, further research is needed to clarify this issue.

The fact that plastic flow occurs upon unloading means that a Bauschinger effect is observed. However, the traditional Bauschinger effect observed in bulk materials refers to samples first deformed, say, in tension, and then in compression with the yield stress in compression being smaller than the initial yield stress in tension. In other words, plastic flow occurs earlier in compression when the sample has been deformed beyond yield in tension. However, the stress–strain curves in Figure 2 are such that reverse plastic flow occurs during unloading even when the stress is still tensile. This is a strong form of the Bauschinger effect, which has also been called "unusual"[30] or "anomalous".[10] This type of Bauschinger effect can be beneficial for fatigue resistance as it reduces damage (dislocation) accumulation during cyclic loading. The strong Bauschinger effect has been previously observed experimentally in micropillars[12] and thin-films[9] when they are coated by hard ceramic films, which act as barriers to dislocation and promote dislocation pile-ups, causing backward flow upon unloading. It has also been observed in polycrystals with heterogeneous grain sizes,[8] where the earlier yielding of large grains leads to internal stresses in the smaller grains, resulting in an asymmetry between loading and unloading. The Bauschinger effect caused by a hard film coating may be regarded as an "extrinsic" effect and may not be beneficial in extending the fatigue life of nanocomposites, because the hard film tends to fracture during cyclic loading, deteriorating the mechanical properties of the material. In contrast, the Bauschinger effect of the pentatwinned nanowires reported here may be regarded as an "intrinsic" effect, ultimately rooted in the crystal geometry of the as-synthesized nanowires and not requiring any post-processing. It is interesting to note that the twin boundaries that are responsible for the strong Bauschinger effect reported here are also responsible for improved ductility of nanotwinned materials[31,32] although the specific mechanisms are different. The mechanistic details on the plastic recovery of pentatwinned nanowires are elaborated in subsequent sections.

In order to quantify the magnitude of the Bauschinger effect, in Figure 3 we plot the strain recovery as a function of the unload strain, both normalized by the yield strain.[9] Experimentally, the yield strain is taken as the 0.2% offset strain. In MD simulations, the yield strain is taken at the onset of dislocation nucleation or dislocation motion. The recovery strain is the difference between the strain that would have occurred under ideal elastic unloading (i.e., extrapolation to zero stress along the dashed line plotted in Figure 2) and the actual strain when the stress has returned to zero. Figure 3 contains both experimental and computational results.

The recovery is present in all the diameters tested and it is of the same order of magnitude within experimental scatter. There seems to be a small increase of recovery strain with decreasing diameter but the size effect is weak. This size effect is consistent with the expectation that dislocations in thinner specimens experience a stronger image force that pulls the dislocations toward the surface. On the other hand, there is a pronounced increase of recovery strain as the unload strain is increased. Similar observations were made in thin films and micropillars.[9,12] Here, a higher recovery with higher unloading strains provides another indirect confirmation of the atomistic mechanisms of plastic deformation in pentatwinned nanowires through SFDs because SFDs, being an arrangement of partial

dx.doi.org/10.1021/nl503237t | Nano Lett. 2015, 15, 139–146

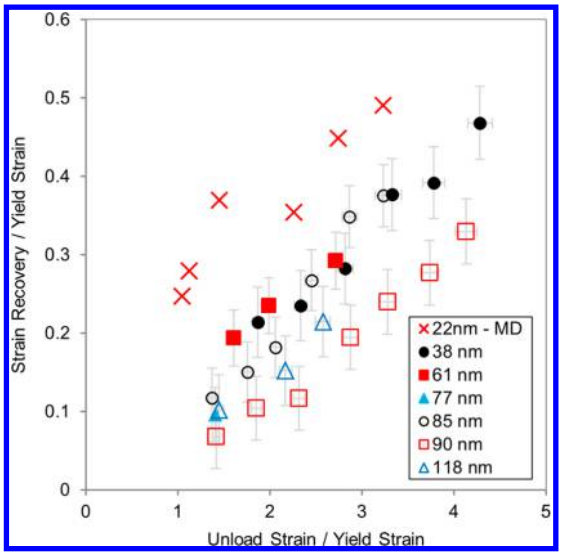

Figure 3. Strain recovery as a function of unloading strain, normalized by the yield strain.

dislocations, become unstable (reversible) upon unloading (see next section) due to their interactions with the twin boundaries, and we have previously observed that increasing tensile strain increases the number of discrete plastic zones, each containing multiple SFDs.[14]

Atomistic Mechanisms. *Simulations and In Situ TEM.* Further insights into the atomistic mechanisms that govern the reversible plastic behavior can be obtained by in situ TEM experiments and MD simulations. Experimentally, we tested a 61 nm nanowire in tension in situ TEM. (A video of the testing process is available in the Supporting Information). To capture the details of the plastic behavior we loaded slowly the nanowire from its initial state at relatively low magnification. In the initial state shown in Figure 4a, the nanowire shows a structure free of dislocations and with some bend contours resulting from slight misalignments between the shuttles of the testing microsystem. After tension to a strain of ∼2.5% we observed the nucleation of a defect, indicated in Figure 4b with a white arrow. After a slight tension to a higher strain (∼2.7%), we stopped the deformation and zoomed in (Figure 4c). Maintaining the same magnification we proceeded to unload and at a strain of ∼2.1% we observed the disappearance of the defect (Figure 4d). Loading the nanowire again promoted the nucleation of the same defect, this time at a strain of ∼2.9% (Figure 4e). This in situ TEM experiment demonstrated the reversible nature of the plastic deformation in these pentatwinned nanowires. However, due to tilting limitations with the TEM holder designed to accommodate the testing microsystem it was not possible to establish unambiguously the dislocation type.

Therefore, to gain more insights into the plastic mechanisms and dislocation activities we analyze the MD simulation snapshots using the Crystal Analysis Tool with OVITO,[33,34] which allows us to identify the type of dislocations formed during tensile straining.

The MD snapshots are shown in Figure 5 in which twin planes are plotted for reference. The dominant dislocations are Shockley partials with Burgers vector 1/6⟨112⟩ and partial dislocations with Burgers vector 1/9⟨222⟩ at the intersection between SFDs and twin boundaries. This observation is expected given our previous prediction that SFD formation is the dominant plastic deformation mechanism in pentatwinned silver nanowires.[14] In particular, each SFD starts with the nucleation of a (leading) Shockley partial at the surface, creating a stacking fault in one of the five single crystal domains. Propagation of the stacking fault into neighboring domains leaves 1/9⟨222⟩ dislocations at the twin boundary (we will call such dislocations through-twin partials). These dislocations can be visualized using the double Thompson tetrahedron, shown in Figure 5a,[35] which represents the

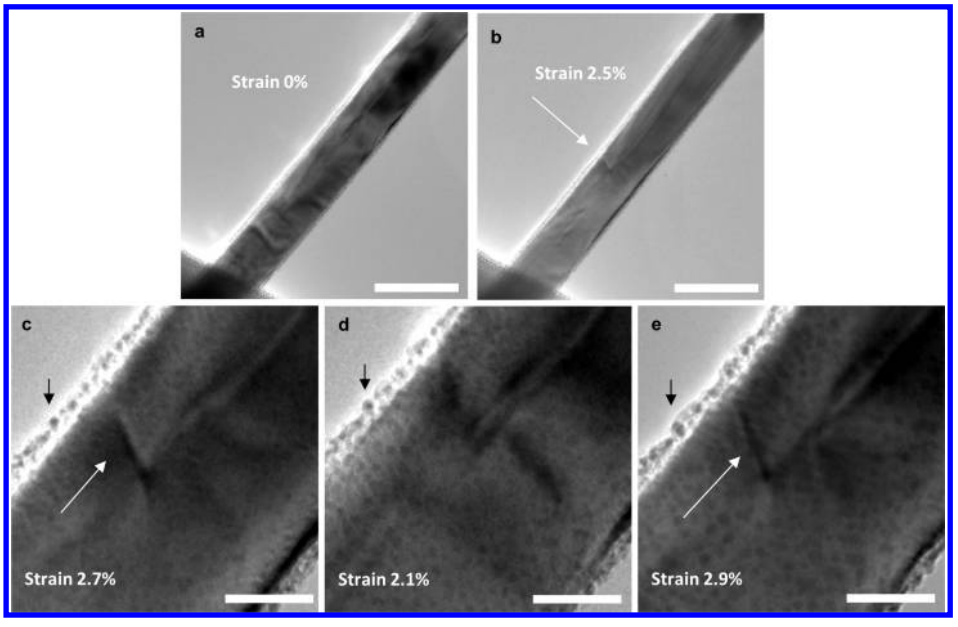

Figure 4. Experimental evidence of reversible plastic deformation. (a) A 61 nm nanowire initially free of dislocations was loaded until a defect nucleation event (b) was observed (white arrow). (c) Subsequently, the loading process was stopped and the defect was imaged at high resolution. Note the black arrow as a point of reference for subsequent images. (d) Keeping the same magnification, unloading is performed, leading to the disappearance of the defect. Scale bars: a-b: 100 nm, c-e: 20 nm. Further loading (e) leads to the nucleation of the defect at the same location.

dx.doi.org/10.1021/nl503237t | *Nano Lett.* 2015, 15, 139−146

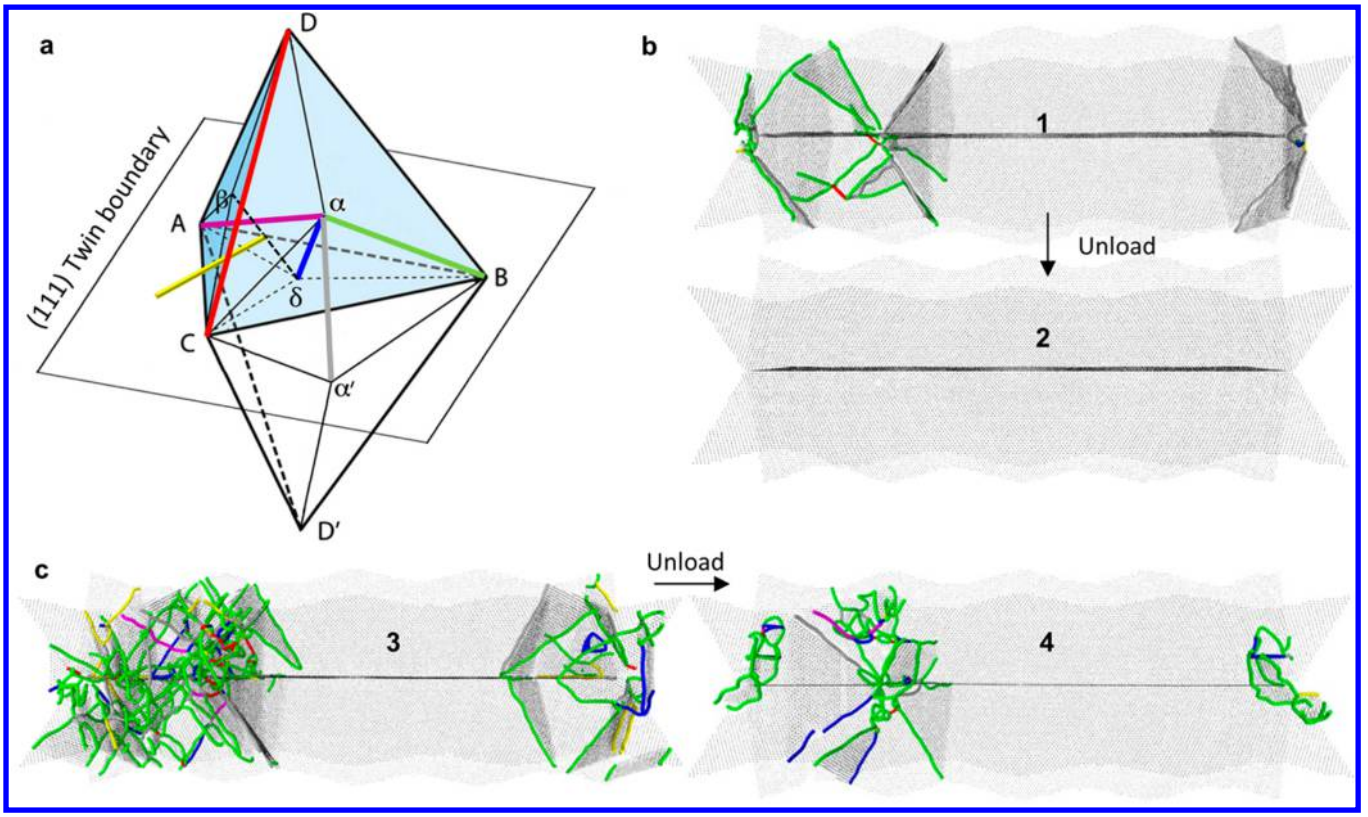

Figure 5. (a) Schematic of the double Thompson tetrahedron used to visualize the Burgers vectors of the dislocations in the pentatwinned structure. The following color convention is used for the MD snapshots: green, Shockley partial; gray, trough twin partial; blue, stair-rod dislocation; purple, Frank partial; yellow, Hirth partial; red, perfect dislocations. (b) MD Snapshots of the 1−2 unloading of Figure 2b, indicating full recovery when only Shockley partial and through-twin dislocations are present in the system. (c) MD Snapshots of the 3−4 unloading of Figure 2b, indicating that full recovery is impeded when Shockley partial and through-twin dislocations are entangled with other dislocations. In the snapshots, only atoms belonging to twin boundaries or stacking faults are visualized as dots, while dislocation lines are colored. Figure 5a reproducted with permission from ref 35. Copyright 2011 Elsevier.

dislocations in a face-centered cubic crystal and their interactions with the {111} twin boundary. In particular, the Burgers vectors of Shockley partials nucleated at the surface of the nanowires have a 30° angle with the twin boundary (e.g., Bα), and those of the through-twin partial dislocation are perpendicular to the twin boundary (e.g., α' α).

Our MD simulations show that these two types of dislocations are highly reversible and hence are responsible for the plastic strain recovery upon unloading. In particular, Figure 5b shows that when these dislocations are the major types of dislocation present, unloading leads to full reversibility and a complete recovery of the plastic strain. Partial plastic recovery occurs as other types of dislocation form to anchor the dislocation network. This is evident in Figure 5c, where Shockley partials, through-twin partials, perfect dislocations, and other dislocations have formed a complex structure. Upon unloading, this entanglement persists at zero stress, thus preventing a full recovery. Our MD simulations show that such complex dislocation structures form when multiple SFDs intersect with each other, although the detailed reaction mechanisms are probably too complex to enumerate in full detail.

To complement the MD simulations results, we calculated the energy barrier of several unit processes involving Shockley and through-twin partials during strain recovery, using a modified version of the string method.[36] For simplicity, we consider the destruction of a five-sided stacking fault hat (SFH, see Figure 6a), which is half of an SFD, during unloading. Several unit processes have been studied (see Supporting Information). It is found that the removal of the first stacking fault area from a five-sided SFH is the rate-limiting step. After the removal of the first face, the removal of the remaining proceeds quickly without any energy barrier (see Supporting Information).

Figure 6b shows that the energy barrier for the removal of the first stacking fault area from a SFH. As the stress is reduced during unloading, the energy barrier becomes very small when the stress is still positive (i.e., tensile). This is consistent with the MD simulation result showing that isolated SFDs formed during loading would be removed during unloading. At the experimental time scale, energy barriers around 0.5 eV can be overcome by thermal fluctuation. This means that a SFH (or SFD) becomes unstable when the stress drops below 0.5 GPa.

The energy barrier results are also consistent with the slope changes in the stress−strain curve, during the unloading process, as predicted by MD (Figure 2b). In the initial stage of unloading, the slope is relatively high, similar to the elastic regime. The slope starts to decrease further when the stress drops below 1 GPa. This is when "perfect" SFHs start to be destroyed. Activation of the process shown in Figure 6 leads to removal of many SFHs that are not pinned by other dislocations, which leads to recovery of plastic strain visible on the stress−strain curves.

dx.doi.org/10.1021/nl503237t | Nano Lett. 2015, 15, 139−146

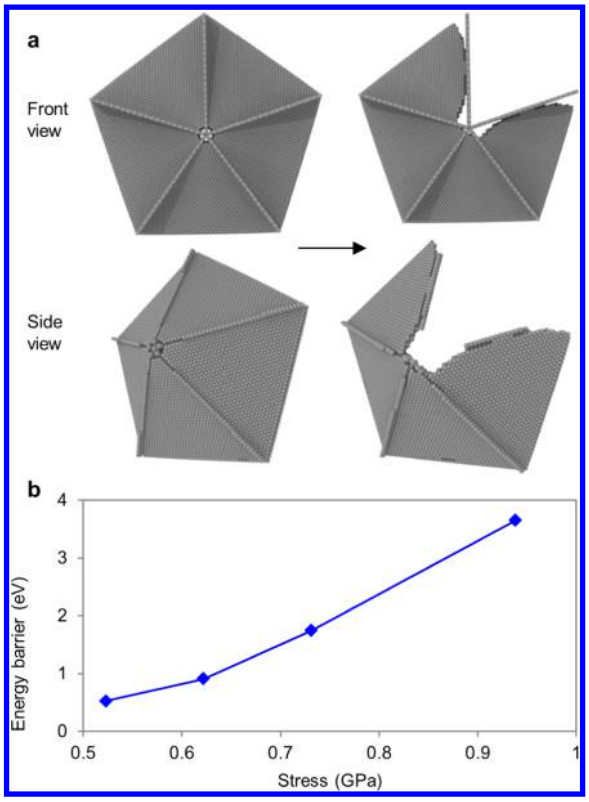

Figure 6. Energy barrier calculations for the rate-limiting process during unloading, that is, the removal of a stacking fault area from a perfect SFH. (a) We selectively visualized atoms with high central symmetry parameter. The stacking fault area is removed when a leading partial exits the SFH, leaving an empty area in the plot. (b) Energy barrier for the process shown in panel a.

Therefore, both the MD simulations and the energy barrier calculations show that the plastic strain recovery is mostly caused by the destruction of SFDs when the applied stress is lowered but still in the tensile regime. However, when dislocations other than the Shockley and through-twin partials appear (due to SFD intersection), part of the dislocation structure become anchored inside the nanowire, leading to incomplete recovery (Figure 5c).

Conclusions. In summary, we have characterized the cyclic plastic behavior of pentatwinned silver nanowires by both in situ electron microscopy experiments and atomistic simulations. Experiments are enabled by a novel MEMS device designed for displacement-controlled testing of nanowires. The experimental and computational results reveal a strong intrinsic Bauschinger effect, i.e., reverse plastic flow during unloading even when the stress remains tensile. Both in situ TEM experiments and MD simulations show that the recovery of plastic strain is caused by reversible dislocation activity. In particular, the deformation mechanism of stacking Fault Decahedron (SFD) formation, which is mediated by Shockley and through-twin partial dislocations, can be reversed when the tensile stress drops below a threshold value. However, when dislocations of different types form through reactions, they can anchor part of the dislocation network even when the stress drops to zero, making the recovery incomplete.

It is of interest to discuss whether the Bauschinger effect reported here can also occur in single crystal nanowires, that is, without the five twin boundaries. Recovery of plastic deformation has been reported by MD simulations of single crystal metal nanowires in torsion[37] in which partial dislocations stored in the nanowires can easily escape during untwist. However, such mechanism is unlikely to occur and has not been reported in single crystal nanowires under uniaxial loading, because dislocations nucleated from the nanowire surface can easily escape from the opposite surface under uniaxial loading, leaving the nanowire in a "dislocation starved" state.[38] On the other hand, reversible deformation can occur in single crystal gold nanowires where plasticity is mediated by deformation twinning.[11] However, the underlying mechanism does not involve dislocation storage and recovery and hence it is not referred to as a Bauschinger effect. Incidentally, computations indicate plastic recovery is possible for nanowires with twins running along the cross section.[39] However, those nanowires only display recovery on a narrow set of strains, specifically before trailing partials nucleate and generate perfect dislocations, and only show this phenomenon under certain twin densities. In contrast to these cases, pentatwinned nanowires show partial recovery more generally, at all strains beyond the plastic regime. Given that SFD formation is a mechanism particular to the pentatwinned atomic structure, we speculate that the intrinsic Bauschinger effect reported here in pentatwinned nanowires may be stronger that in nontwinned nanostructures, such as single crystal nanowires.

The partial recovery of plastic deformation in the pentatwinned nanowires is an important aspect to take into account for the design of nanowire-based flexible electronic applications where cyclic deformation of the nanowires past the yield point is likely to happen. In particular, a natural extension of this work could be made to study the fatigue life of the nanowires, given the relation between fatigue life and accumulation of plastic deformation. In particular, if fatigue stresses are all of the same sign (tensile), the observed plastic recovery should be beneficial to fatigue life. Further research with combined tensile and compressive loading is needed to clarify the effect of load-direction reversal on fatigue.

Methods. *Electronic Setup Used in the Experiments.* Cyclic straining was achieved by programming a waveform containing several cycles of increasing and decreasing voltage in a signal generator and using such waveform to actuate the thermal actuator. The electronics for load sensing and feedback were implemented using a commercial chip for capacitive sensing (MS3110), an analog feedback control with fast response (100 kHz, Stanford Research Systems SIM960) and voltage amplifiers (OPA445). The MEMS device was wire-bonded to a custom printed-circuit-board (PCB) that allows operation of the MEMS inside electron microscopes.[24]

Experimental Data Reduction for the Stress–Strain Curves. Strain was determined from the applied voltage to the thermal actuator and a calibration curve obtained before the experiment with no specimen mounted. Given that the other end of the specimen remains stationary and the actuator displacement is solely controlled by the applied voltage,[24] the nanowire deformation is equal to the actuator displacement. The force is derived from the control voltage applied to the electrostatic actuator and the actuator geometry.[24] To obtain stress, this force is divided by the initial nanowire cross-section, which was assumed to be of circular shape.[14] The diameter was determined by a high-resolution image of the nanowire. The data acquisition rate was 1000 Hz, and a moving average with a window of 20 data points was applied to filter out noise.

dx.doi.org/10.1021/nl503237t | *Nano Lett.* 2015, 15, 139–146

■ ASSOCIATED CONTENT

Supporting Information

All the experimental stress−strain curves, more detailed energy barrier calculations, and a video of the TEM test are included. This material is available free of charge via the Internet at http://pubs.acs.org.

■ AUTHOR INFORMATION

Corresponding Authors

*E-mail: espinosa@northwestern.edu.

*E-mail: caiwei@stanford.edu.

Author Contributions

R.B. performed and analyzed the experiments. A.A. performed the MD simulations. S.L. and S.R. performed the energy barrier calculations. K.S. and J.H. synthesized the silver nanowires. H.E. conceived the research. H.E. and W.C. provided guidance throughout the research. R.B., A.A., S.R., W.C., and H.E. cowrote the paper.

R.A.B. and A.A. contributed equally.

Notes

The authors declare no competing financial interest.

■ ACKNOWLEDGMENTS

H.D.E. gratefully acknowledges support from NSF through award No. DMR-0907196. We thank Dr. Shuyou Li for help with TEM imaging and Rajaprakash Ramachandramoorthy for sample preparation of silver nanowires. We also thank Prof. Ting Zhu from Georgia Tech for helpful discussions on atomistic modeling. This work made use of the EPIC facility (NUANCE Center-Northwestern University), which has received support from the MRSEC program (NSF DMR-1121262) at the Materials Research Center, and the Nanoscale Science and Engineering Center (EEC-0118025/003), both programs of the National Science Foundation; the State of Illinois; and Northwestern University. This work was partly supported by the U.S. Department of Energy, Office of Basic Energy Sciences, Division of Materials Sciences and Engineering under Award No. DE-SC0010412 (A.A. and W.C.). S. R. acknowledges the support by Basic Science Research Program through the National Research Foundation of Korea (NRF) funded by the Ministry of Science, ICT & Future Planning (2013R1A1A010091).

■ REFERENCES

(1) Xu, F.; Zhu, Y. Highly Conductive and Stretchable Silver Nanowire Conductors. *Adv. Mater.* **2012**, *24* (37), 5117−5122.

(2) Song, L.; Myers, A. C.; Adams, J. J.; Zhu, Y. Stretchable and Reversibly Deformable Radio Frequency Antennas Based on Silver Nanowires. *ACS Appl. Mater. Interfaces* **2014**, *6* (6), 4248−4253.

(3) Amjadi, M.; Pichitpajongkit, A.; Lee, S.; Ryu, S.; Park, I. Highly Stretchable and Sensitive Strain Sensor Based on Silver Nanowire−Elastomer Nanocomposite. *ACS Nano* **2014**, *8* (5), 5154−5163.

(4) Choi, H. O.; Kim, D. W.; Kim, S. J.; Yang, S. B.; Jung, H.-T. Role of 1D Metallic Nanowires in Polydomain Graphene for Highly Transparent Conducting Films. *Adv. Mater.* **2014**, 5475−4581.

(5) Lee, J.; Lee, I.; Kim, T.-S.; Lee, J.-Y. Efficient Welding of Silver Nanowire Networks without Post-Processing. *Small* **2013**, *9* (17), 2887−2894.

(6) Patel-Predd, P. The trouble with touch screens. *IEEE Spectrum* **2009**, *46* (1), 11−12.

(7) Bourzac, K. Nanomaterials Could Enable Large, Flexible Touch Screens. *MIT Technol. Rev.* **2014**.

(8) Rajagopalan, J.; Rentenberger, C.; Karnthaler, H. P.; Dehm, G.; Saif, M. T. A. In situ TEM study of microplasticity and Bauschinger effect in nanocrystalline metals. *Acta Mater.* **2010**, *58* (14), 4772−4782.

(9) Xiang, Y.; Vlassak, J. J. Bauschinger effect in thin metal films. *Scr. Mater.* **2005**, *53* (2), 177−182.

(10) Liu, D. B.; He, Y.M.; Dunstan, D.J.; Zhang, B.; Gan, Z.P.; Hu, P.; Ding, H.M. Anomalous Plasticity in the Cyclic Torsion of Micron Scale Metallic Wires. *Phys. Rev. Lett.* **2013**, *110*, 244301.

(11) Lee, S.; Im, J.; Yoo, Y.; Bitzek, E.; Kiener, D.; Richter, G.; Kim, B.; Oh, S.H. Reversible cyclic deformation mechanism of gold nanowires by twinning-detwinning transition evidenced from in situ TEM. *Nat. Commun.* **2014**, *5*, 3033.

(12) Jennings, A. T.; Gross, C.; Greer, F.; Aitken, Z. H.; Lee, S. W.; Weinberger, C. R.; Greer, J. R. Higher compressive strengths and the Bauschinger effect in conformally passivated copper nanopillars. *Acta Mater.* **2012**, *60* (8), 3444−3455.

(13) Greer, J. R.; De Hosson, J. T. M. Plasticity in small-sized metallic systems: Intrinsic versus extrinsic size effect. *Prog. Mater. Sci.* **2011**, *56* (6), 654−724.

(14) Filleter, T.; Ryu, S.; Kang, K.; Yin, J.; Bernal, R. A.; Sohn, K.; Li, S. Y.; Huang, J. X.; Cai, W.; Espinosa, H. D. Nucleation-Controlled Distributed Plasticity in Penta-twinned Silver Nanowires. *Small* **2012**, *8* (19), 2986−2993.

(15) Weinberger, C. R.; Cai, W. Plasticity of metal nanowires. *J. Mater. Chem.* **2012**, *22* (8), 3277−3292.

(16) Zhu, Y.; Qin, Q.Q.; Xu, F.; Fan, F.R.; Ding, Y.; Zhang, T.; Wiley, B.J.; Wang, Z.L. Size effects on elasticity, yielding, and fracture of silver nanowires: In situ experiments. *Phys. Rev. B* **2012**, *85*, 045443.

(17) Zhang, Y.; Liu, X.; Ru, C.; Zhang, Y. L.; Dong, L.; Sun, Y. Piezoresistivity Characterization of Synthetic Silicon Nanowires Using a MEMS Device. *J. Microelectromech. Syst.* **2011**, *PP* (99), 1−9.

(18) Zhang, D. F.; Breguet, J. M.; Clavel, R.; Sivakov, V.; Christiansen, S.; Michler, J. Electron Microscopy Mechanical Testing of Silicon Nanowires Using Electrostatically Actuated Tensile Stages. *J. Microelectromech. Syst.* **2010**, *19* (3), 663−674.

(19) Brown, J. J.; Baca, A. I.; Bertness, K. A.; Dikin, D. A.; Ruoff, R. S.; Bright, V. M. Tensile measurement of single crystal gallium nitride nanowires on MEMS test stages. *Sens. Actuators, A* **2011**, *166* (2), 177−186.

(20) Guo, H.; Chen, K.; Oh, Y.; Wang, K.; Dejoie, C.; Asif, S. A. S.; Warren, O. L.; Shan, Z. W.; Wu, J.; Minor, A. M. Mechanics and Dynamics of the Strain-Induced M1-M2 Structural Phase Transition in Individual VO_2 Nanowires. *Nano Lett.* **2011**, *11* (8), 3207−3213.

(21) Cheng, G. M.; Chang, T. H.; Qin, Q. Q.; Huang, H. C.; Zhu, Y. Mechanical Properties of Silicon Carbide Nanowires: Effect of Size-Dependent Defect Density. *Nano Lett.* **2014**, *14* (2), 754−758.

(22) Espinosa, H. D.; Zhu, Y.; Moldovan, N. Design and operation of a MEMS-based material testing system for in-situ electron microscopy testing of nanostructures. *J. Microelectromechan. Syst.* **2007**, *16* (5), 1219−1231.

(23) Soer, W. A.; De Hosson, J. T. M.; Minor, A.M.; Shan, Z.; Asif, S. A. S.; Warren, O.L. Incipient plasticity in metallic thin films. *Appl. Phys. Lett.* **2007**, *90*, 181924.

(24) Pantano, M.; Bernal, R.; Pagnotta, L.; Espinosa, H. Multiphysics design and implementation of a microsystem for displacement-controlled tensile testing of nanomaterials. *Meccanica* **2014**, 1−12.

(25) Zhu, Y.; Corigliano, A.; Espinosa, H. D. A Thermal Actuator for Nanoscale In-situ Microscopy Testing: Design and Characterization. *J. Micromechan. Microeng.* **2006**, *16*, 242−253.

(26) MD++. Available from: http://micro.stanford.edu/MDpp/ (accessed October 14, 2014).

(27) LAMMPS. Available from: http://lammps.sandia.gov/ (accessed October 14, 2014).

(28) Williams, P. L.; Mishin, Y.; Hamilton, J. C. An embedded-atom potential for the Cu-Ag system. *Modell. Simul. Mater. Sci. Eng.* **2006**, *14* (5), 817−833.

(29) Agrawal, R.; Peng, B.; Espinosa, H. D. Experimental-Computational Investigation of ZnO nanowires Strength and Fracture. *Nano Lett.* **2009**, *9* (12), 4177−4183.

(30) Xiang, Y.; Vlassak, J. J. Bauschinger and size effects in thin-film plasticity. *Acta Mater.* **2006**, *54* (20), 5449−5460.
(31) Lu, K.; Lu, L.; Suresh, S. Strengthening Materials by Engineering Coherent Internal Boundaries at the Nanoscale. *Science* **2009**, *324* (5925), 349−352.
(32) Wei, Y. J.; Li, Y.Q.; Zhu, L.C.; Liu, Y.; Lei, X.Q.; Wang, G.; Wu, Y.X.; Mi, Z.L.; Liu, J.B.; Wang, H.T.; Gao, H.J. Evading the strength-ductility trade-off dilemma in steel through gradient hierarchical nanotwins. *Nat. Commun.* **2014**, *5*, 3580.
(33) Stukowski, A.; Bulatov, V.V.; Arsenlis, A. Automated identification and indexing of dislocations in crystal interfaces. *Modell. Simul. Mater. Sci. Eng.* **2012**, *20*, 085007.
(34) Stukowski, A.; Albe, K. Extracting dislocations and non-dislocation crystal defects from atomistic simulation data. *Modell. Simul. Mater. Sci. Eng.* **2010**, *18*, 085001.
(35) Zhu, Y. T.; Wu, X. L.; Liao, X. Z.; Narayan, J.; Kecskes, L. J.; Mathaudhu, S. N. Dislocation-twin interactions in nanocrystalline fcc metals. *Acta Mater.* **2011**, *59* (2), 812−821.
(36) Ryu, S.; Kang, K.; Cai, W. Entropic effect on the rate of dislocation nucleation. *Proc. Natl. Acad. Sci. U.S.A.* **2011**, *108* (13), 5174−5178.
(37) Weinberger, C. R.; Cai, W. Orientation-Dependent Plasticity in Metal Nanowires under Torsion: Twist Boundary Formation and Eshelby Twist. *Nano Lett.* **2010**, *10* (1), 139−142.
(38) Greer, J. R.; Nix, W.D. Nanoscale gold pillars strengthened through dislocation starvation. *Phys. Rev. B* **2006**, *73*, 245410.
(39) Deng, C.; Sansoz, F. Enabling Ultrahigh Plastic Flow and Work Hardening in Twinned Gold Nanowires. *Nano Lett.* **2009**, *9* (4), 1517−1522.